International Journal of Soft Computing 8 (2): 118-125, 2013
ISSN: 1816-9503

Implementation of Genetic Fuzzy Controller for Harmonic Analysis of Quasi Resonant Converters Fed Drive

[1]M. Ranjani and [2]P. Murugesan
[1]Department of Electrical and Electronics Engineering,
Sathyabama University, Chennai, Tamil Nadu, India
[2]Department of Electrical and Electronics Engineering, S.A. Engineering College,
Chennai, Tamil Nadu, India

Abstract: This study presents a comparative harmonic analysis between a ZCS-QRC and ZVS-QRC topologies fed DC drive that uses a genetic fuzzy controller. The advantages of the different topologies employing MOSFET's are presented. This operation employing genetic fuzzy controller can reduce the harmonic distortion and improves the performance of the drive when compared with the conventional control methods. The main objective of this research is to obtain reduced transient response, reduced switching stresses and switching losses which in turn enhances the efficiency and commutation capability of motor.

Key words: Fuzzy Logic Controller (FLC), Zero Current Switching Quasi-Resonant Converter (ZCS-QRC), Zero Voltage Switching Quasi-Resonant Converter (ZVS-QRC), Genetic Algorithm (GA), Total Harmonic Distortion (THD), Direct Current (DC)

INTRODUCTION

In Direct Current (DC) motor when armature current is commutated, the current ripple is generated due to the stator winding inductance and deviation of back emf from its characteristics. This current ripples leads to disturbances in control applications. The DC motor drives have the advantage of high controllability and are used in many applications such as robotic manipulators, position control, steel mining and paper and textile industries. In some industrial applications, the dynamic response of drives is bounded by certain limitations such as transient time and steady state error. In addition when they are fed from PWM converter (Mohan *et al*., 1995) they suffer from high switching losses, reduced reliability, electromagnetic inference and acoustic noise. To overcome the above difficulties Quasi-resonant converters (Liu and Lee, 1990) are used which can be either Zero Current (ZC) or Zero Voltage switching (ZV). In order to improve the speed response and regulation of the converter fed drives it is necessary to have closed loop control.

Conventional controllers namely PI controllers are designed on the basis of local linearization about an operating condition. But they are ineffective when the speed command and load changes have huge variations also the system cannot be operated far away from the linearizing point. In industrial application, the drive is forced to operate under wide range of load characteristics and the parameters vary extensively. Thus, a modern control is needed to ensure a specific dynamic response independent of parameter variations, variations in speed command and load disturbances.

In this study, the advent of FLC has been suggested as an alternative approach to conventional control techniques for complex control system like non linear system. The design of FLC does not require the exact mathematical model of the system and can compensate the parameter variation due to load disturbances (Kandel and Langholz, 1994; Kung and Liaw, 1994). Unfortunately, a good performance cannot be obtained for incorrect membership functions, fuzzy rules and scaling factors. This necessitates the optimization technique of FLC by Genetic algorithm (Reznik, 1997; Hu *et al*., 1997; Tan and Hu, 1997; Mohammadian and Stonier, 1994) to achieve optimal solutions of membership function, fuzzy rules and scaling factors.

In this study, the harmonic analysis has been carried out for two configurations namely (series and parallel) ZCS-QRC and ZVS-QRC. The two QRC's are employed for speed control of DC drive which employs FLC and GA based FLC as feedback loop.

MODELING OF ZCS QRC AND ZVS QRC

Analysis of ZCS QRC: The QRC with ZCS topology considered for the present research comprises of two

Corresponding Author: M. Ranjani, Department of Electrical and Electronics Engineering, Sathyabama University, Chennai, Tamil Nadu, India

configuration namely Series (L-type) ZCS QRC and Parallel (M-type) ZCS QRC. To analyze its behavior, the following assumptions are made:

- Armature inductance is much larger than resonant inductance
- The DC motor is treated as a constant current sink
- Semiconductor switches are ideal
- Reactive elements of the tank circuit are ideal

A switching cycle can be divided into four stages. Suppose that before MOSFET turns on, diode carries the steady-state output current I_a and capacitor voltage V_{cr} is clamped at zero. At time t_0, MOSFET turns on, starting a switching cycle.

Design of series ZCS QRC fed drive: A switching cycle can be divided into four stages. Suppose that before MOSFET turns on, diode carries the steady-state output current I_a and capacitor voltage V_{cr} is clamped at zero. At time t_0, MOSFET turns on, starting a switching cycle. Figure 1 shows the half wave series ZCS QRC and Fig. 2 shows the simulated waveform of series ZCS QRC.

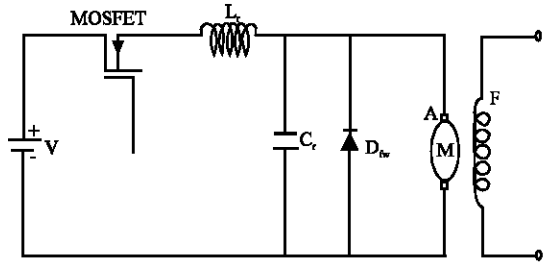

Fig. 1: ZCS-half wave series quasi-resonant converter

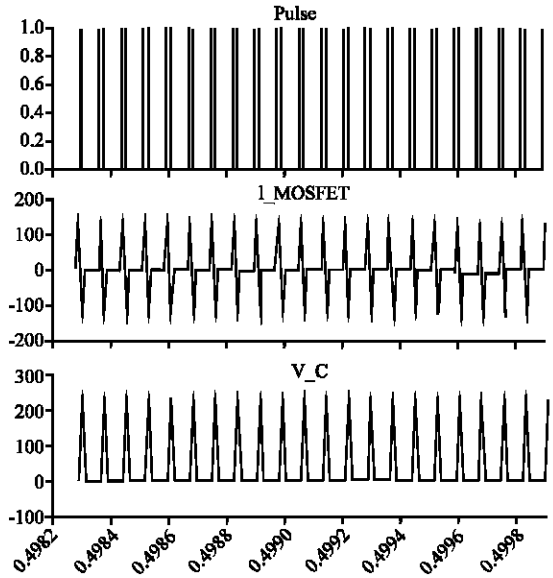

Fig. 2: Waveforms for halfwave series ZCS-QRC

Mode 1 (linear stage [t_0, t_1]): Input current i_{Lr} rises linearly and its waveform is governed by the state equation:

$$L_r\left(\frac{di_{Lr}}{d_t}\right)=E \tag{1}$$

the duration of this stage t_{d1} (= t_1-t_0) can be solved with boundary conditions of $I_{Lr}(0) = 0$ and $I_{Lr}(t_{d1}) = I_a$, thus:

$$t_{d1}=\frac{(L_r I_a)}{E} \tag{2}$$

Mode 2 (resonant stage [t_1, t_2]): At time t_1, the input current rises to the level of I_a, freewheeling diode is commutation off and the difference between the input current and the output current $i_{Lr}(t)$-I_a flows into C_r as can be seen from Fig. 1 voltage V_{cr} rises in a sinusoidal fashion. The state equations are:

$$C_r\left(\frac{dV_{cr}}{dt}\right)=I_{Lr}(t)-I_a \tag{3}$$

$$L_r\left(\frac{di_{Lr}}{dt}\right)=E-V_{cr}(t) \tag{4}$$

with initial conditions $V_{cr}(0) = 0$, $i_{Lr}(0) = I_a$ therefore,

$$i_{Lr}(t)=I_a+\left(\frac{E}{Z_0}\right)\sin\omega t \tag{5}$$

$$V_{cr}(t)=E(1-\cos\omega t) \tag{6}$$

Mode 3 (recovering stage [t_2, t_3]): Since, MOSFET is off at time t_2, capacitor begins to discharge through the output loop and V_{cr} drops linearly to zero at time t_3 as shown in the Fig. 2. The state equation during this interval is:

$$C_r\left(\frac{dV_{cr}}{dt}\right)=-I_a \tag{7}$$

The duration of this stage t_{d3} (= t_3-t_2) can be solved with the initial condition $V_{cr}(0) = V_{cr}$:

$$t_{d3}=\frac{C_r V_{cr}}{I_a} \tag{8}$$

$$t_{d3}=\frac{C_r E(1-\cos\alpha)}{I_a} \tag{9}$$

Mode 4 (freewheeling stage [t_3, t_4]): After t_3, output current flows through diode. The duration of this stage is t_{d4} (= t_4−t_3) and:

$$t_{d4} = T_s - t_{d1} - t_{d2} - t_{d3} \quad (10)$$

where, T_s is the period of the switching cycle. After an interval of Toff, during which It is zero and V_{cr} = 0, the gate drive to the MOSFET is again applied at T4 to turn it on and the operation during the next cycle is similar to that of the preceding cycle. By controlling the dead time (T4-T3) the average value of the armature voltage and hence the speed of the dc motor can be controlled:

- Characteristic impedance:

$$Z_n = \sqrt{\left(\frac{L_1}{C_1}\right)}$$

- Resonant angular frequency:

$$\omega = \frac{1}{\sqrt{(L_1 C_1)}}$$

- Resonant frequency:

$$f_n = \frac{\omega}{2\Pi}$$

Design of parallel ZCS QRC fed drive: A switching cycle can be divided into four stages. Assume that initially the diode carries the armature current I_a, the resonant capacitor voltage equals E and the MOSFET is off. Figure 3 shows the half wave parallel ZCS QRC and Fig. 4 shows the simulated waveform of parallel ZCS QRC.

Inductor charging state (t_0, t): At the beginning of switching cycle, t = t_0, the MOSFET is turned on. The entire input voltage E appears across L_r and the current I_t builds up linearly until it equals I_a at t_1. The current i_{Lr} is governed by the state equation:

$$\frac{L_r di_{Lr}}{dt} = E \quad (11)$$

The duration of stage 1, t_{d1} (t_1-t_0) can be solved with boundary conditions i_{Lr} (0) = 0 and i_{Lr} (t_{d1}) = I_a. Thus:

$$T_{d1} = \frac{L_r I_a}{E} \quad (12)$$

Resonant stage (t_1, t_2): At t_1 the current i_T equals I_a and this cause the diode to stop conducting. Now, L_r and Cr form a parallel resonant circuit. At t_1', i_T reaches its peak value and V_{cr} reaches zero. The negative peak of V_{cr} occurs at t_1'' when i_T = I_a. The state equation are:

$$\frac{C_r dV_{cr}}{dt} = i_L(t) - I_a \quad (13)$$

$$\frac{L_r di_{Lr}}{dt} = V_{cr}(t) \quad (14)$$

With the initial conditions $V_{cr}(0)$ = E , $i_{Lr}(0)$ = I_a:

$$i_{Lr}(t) = \frac{I_a + E}{Z_0 \sin(\omega_0 t)} \quad (15)$$

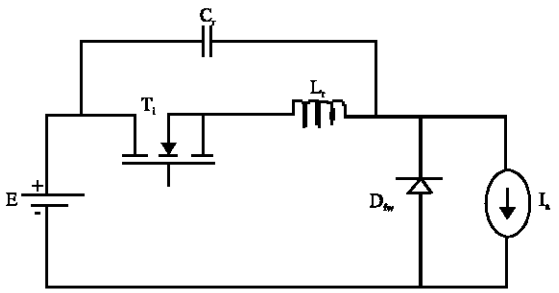

Fig. 3: ZCS-half-wave parallel Quasi-resonant converter

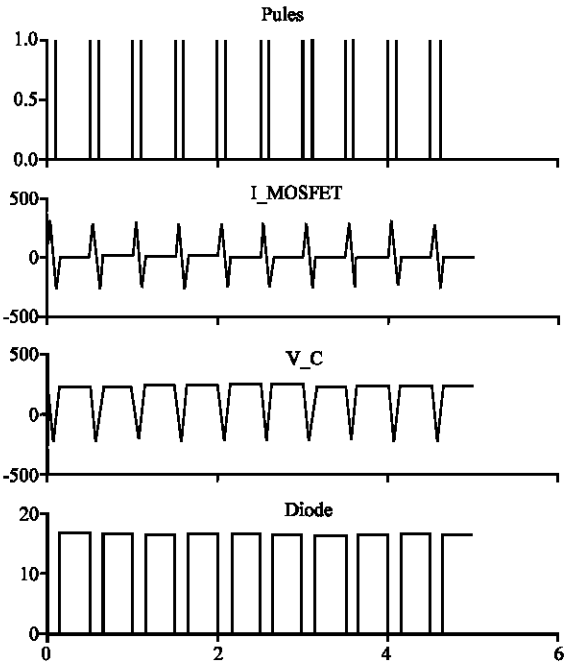

Fig. 4: Waveforms of ZCS-parallal QRC in half wave mode

Where:

$$Z_0 = \sqrt{\frac{L}{C}}$$

$$\omega_0 = \frac{1}{\sqrt{(LC)}}$$

$$V_{cr}(t) = E\sin(\omega_0 t) \quad (16)$$

The duration of stage 2, t_{d2} can be resolved by setting $i_{Lr}(t_{d2}) = 0$. Thus:

$$t_{d2} = \frac{\alpha}{\omega_0} \quad (17)$$

Where:

$$\alpha = \sin^{-1}\left(\frac{-Z_0 I_a}{E}\right)$$

At time t_2, V_{cr} can be solved by using $V_{cr}(t_{d2}) = E\cos\alpha$. The switch naturally turned off since i_T reaches zero at t_2.

Capacitor charging stage (t_2, t_3): Beyond t_2, the base drive for the MOSFET is removed. Now I_a flows through C_r and V_{cr} rises linearly to E at t_3. The state equation during this interval is:

$$\frac{C_r dV_{cr}}{dt} = I_a \quad (18)$$

The duration of stage 3 can be solved with the condition $V_{cr}(0) = E\cos\alpha$:

$$t_{d3} = \frac{C_r E\cos\alpha}{I_a}$$

Freewheeling stage (t_3, t_4): At t_3, the diode turns on and the capacitor voltage stays at E. The armature current freewheels through the diode. The duration of stage 4 is t_{d4}:

$$t_{d4} = T_s - t_{d1} - t_{d2} - t_{d3} \quad (19)$$

where, T_s is the period of a switching cycle. After an interval of t_{offS} during which i_T is zero and $V_{cr} = E$, the base drive to the MOSFET is again applied at t_4 to turn it on and the operation during the next cycle is similar to that of the preceding cycle. It may be seen from the waveforms that the forward switch voltage is limited to E. By controlling the dead time (t_4-t_3), the average value of armature voltage and hence the speed of the DC motor can be controlled.

Design of ZVS QRC fed drive

Analysis of ZVS-QRC: The circuit diagram of buck-boost ZVS QRC (Arulselvi and Govindarajan, 2007) is shown in Fig. 5. The main switch S_1 and an auxiliary switch S_2 are connected in parallel with C_r and L_r, respectively. The conduction time of the main switch S1 decides the buck or boost operation of the converter. The resonant inductor L_r and resonant capacitor C_r form the resonant tank circuit and they are used to shape the voltage waveform across the main switch S_1 in Quasi-sinusoidal form. The effect of C_{ds} of S_1 and S_2 is not considered for resonance of buck-boost ZVS-QRC. D_m is a freewheeling diode, L_m, a magnetizing inductor and C_f, a filter capacitor. The filter capacitor is used to minimize the ripples in the output voltage. Both the switches operate under zero voltage condition.

The converter works in six different modes of operation in a switching cycle. The theoretical resonant waveforms of the converter for different modes under the steady state condition are shown in Fig. 6. It is seen that the switching cycle in ZVS topology starts with the main switch S_1 in the non-conduction state. Six modes of operation are explained by referring to Fig. 1 and 2. During mode 1 [t_0 t_1] the resonant capacitor voltage V_{Cr}

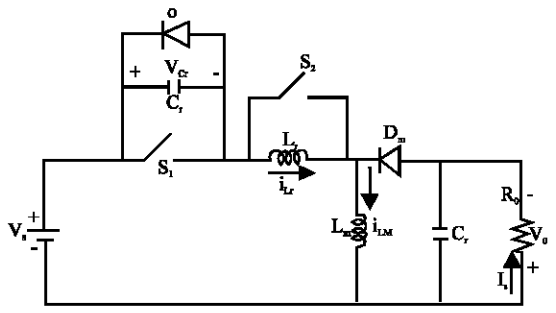

Fig. 5: Half-wave ZVS-QRC

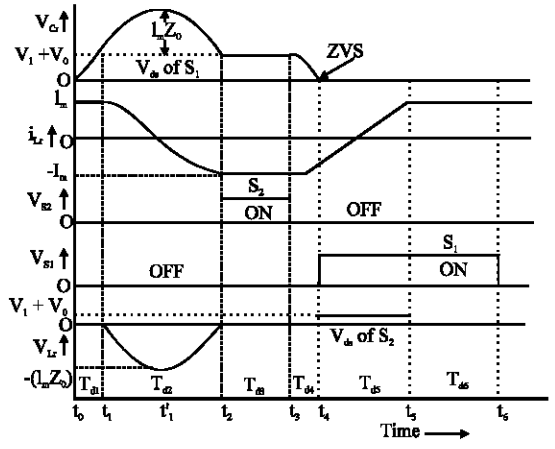

Fig. 6: Resonant waveforms of ZVS-QRC

(V_{ds} of S_1) charges linearly from 0 to $V_s + V_0$ and the inductor current i_{Lr} is maintained constant at I_m. During mode 2 [t_1 t_2] the circuit enters into resonant stage. The resonant capacitor C_r and the resonant inductor L_r resonate together. The capacitor voltage reaches the peak value of I_mZ_0 when i_{Lr} reaches zero. When the capacitor starts discharging, the inductor current has a negative value. At the end of this mode the inductor current reaches its negative peak ($-I_m$) and the capacitor voltage drops to $V_s + V_0$. During mode 3 [t_2, t_3], the switch S_2 is turned on. The resonant capacitor voltage V_{Cr} and resonant inductor current i_{Lr} are kept constant during this mode. Switch S_2 operates under zero voltage condition, since V_{Lr} (V_{ds} of S_2) is zero during this stage. This provides inductor freewheeling which helps in reducing switching frequency band required to regulate the output voltage. The resonant capacitor voltage discharges and reaches zero at the end of mode 4 [t_4 t_5]. As soon as V_{Cr} becomes zero, the main switch S_1 is turned on to ensure zero voltage switching. The main switch S_1 is kept on during modes 5 and 6. The inductor current i_{Lr} charges linearly and reaches I_m at the end of Mode 5. The power transfer to the load takes place during modes 5 and 6. During mode 6, i_{Lr} is maintained constant at I_m and the cycle repeats.

DC voltage transfers gain and the control characteristics of ZVS-QRC: The dc voltage transfer gain (M) of the converter as a function of normalized load Resistance (R) and switching frequency (fs) can be derived by equating the input Energy (E_{in}) and output Energy (E_0) over a complete switching cycle as:

$$E_m = E_0 \tag{20}$$

The total input energy over one switching cycle is given by:

$$E_{in} = \int_0^{T_s} i_{in} V_s \, dt = \int_0^{T_{d1/2}} i_{Lr} V_s dt = \int_0^{T_{d6}} i_L \, V_s \, dt \tag{21}$$

$$E_m = I_m V_s \left[\frac{T_{d1}}{2} + T_{d6} \right]$$

where, T_{dl} and T_{d6} are the time intervals during modes 1 and 6 as shown in Fig. 2. The output energy over one cycle is obtained by evaluating (Eq. 3):

$$E_{in} = \int_0^{T_s} i_0 V_0 \, dt = I_0 V_0 T_s \tag{22}$$

From the conservation of energy theory, equating the input and output energy expressions to calculate the voltage transfers gain (M) of the converter, the gain M with respect to circuit parameters is given by Eq. 4:

$$M = 1 - \left\{ \frac{1}{\left(\frac{fs}{2f_0\pi} \right) \left(\alpha + \left(\frac{R}{2M} \right) \right) + \left(\frac{M}{R} \right) (1 - \cos\alpha) + \frac{2T_{d3}}{T_s}} \right\} \tag{23}$$

Where:

T_{d3} = Holding time or ON time of S2
T_s = Switching period
R_0 = Load resistance

$$\alpha = \pi + \sin^{-1}\left(\frac{(V_s + V_0)}{I_m Z_0} \right); \; \pi \le \alpha \le \frac{3\pi}{2} \tag{24}$$

Characteristic impedance:

$$Z_n = \sqrt{\left(\frac{L_r}{C_r} \right)} \tag{25}$$

Resonant angular frequency:

$$\omega_0 = \frac{1}{\sqrt{(L_r C_r)}} \tag{26}$$

Resonant frequency:

$$f_0 = \frac{1}{2\pi\sqrt{(Lr C_r)}} \tag{27}$$

Normalized load resistance:

$$R = \frac{R_0}{Z_0} \tag{28}$$

The value of M can be varied either by varying f_s or T_{d3}. It has been found by analysis that with the auxiliary switch S_2 set for maximum conduction time (T_{d3}), the range of switching frequency required for the control of output voltage becomes less. However, it has been increased for the same load variation when no auxiliary switch (S_2) is present in the converter.

DESIGN OF FUZZY LOGIC CONTROLLER

The fuzzy logic controller block contains a reference to a fuzzy logic inference system. The inference system

has three linguistic variables which are the two inputs (error signal and error derivative) and the output (control signal). The fuzzy logic inference system for the fuzzy proportional-derivative controller contains a set of fuzzy logic rules that define the behavior of the system in relation between the error signal, error derivative signal and the control signal of the controller. The first input to the fuzzy logic inference system is the error signal which is the difference between the desired speed and the actual speed of the motor. The error integrator signal is achieved by integrating the error signal before passing it to the fuzzy logic controller block. Since, the fuzzy logic controller block expects two inputs, a multiplexer is used to combine the error signal and the error integrator signals as input into the block. The control signal output of the fuzzy logic controller (Mattavelli *et al*., 1997; Bose, 1994; Balestroni *et al*., 2000) is passed as the input of the DC motor block to determine the speed of the motor. The output of the DC motor block which is the motor speed is monitored using a scope to examine its response. The desired speed of the motor is set to a unit constant value to serve a step response input to the system. The error signal of the system is also monitored using a scope. The tuning of the fuzzy logic controller can be achieved by either adjusting the range of the universe of discourse for the linguistic variables, adjusting the input and output scaling gains of the controller or adjusting the number, type and positions of the membership functions used. The Simulink Model of GA-FLC with inclusion of IAE is as shown in Fig. 7. The rules for the fuzzy inference system are shown in Table 1.

GA optimized FLC: The Genetic Algorithm (GA) is employed to perform a comprehensive and complete search in finding an optimal set of solution for the fuzzy logic rules, membership functions and scaling gains for the specified fuzzy is re-implemented but the only difference this time is thatis optimized. The fuzzy inference system consists of three linguistic variables (two inputs and one output) each 25 is rule fuzzy inference system with inputs as the error and the rate of change in error.

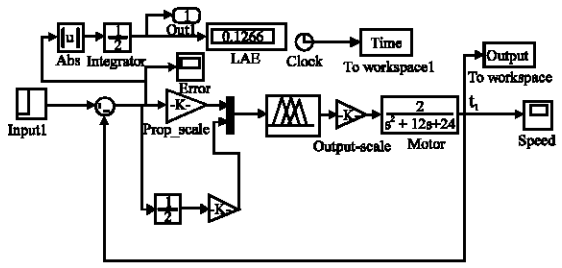

Fig. 7: Simulink Model of GA-FLC with IAE

Table 1: Rule table with 25 rules

	e (t)				
u (t)	NB	NS	Z	PS	PB
de (t)					
NB	NB	NB	NS	NS	Z
NS	NB	NS	NS	Z	PS
Z	NS	NS	Z	PS	PS
PS	NS	Z	PS	PS	PB
PB	Z	PS	PS	PB	PB

Table 2: GA-FLC parameters

Parameters	Values
Population size	30.0
Termination generation	70.0
Crossover probablity	0.6
Mutation probability	0.1

The output of the fuzzy logic inference system is the control action of the controller and the universe of discourse of all the variables are set within the range (-1, 1). The genetic algorithm technique employed in this study is used to tune the fuzzy logic controller (Ko *et al*., 2006; Bucci *et al*., 2000). The tuning approach employs the use of MATLAB M-files and functions to manipulate the fuzzy inference system and scaling gains, run the simulink based simulation, check the resulting performance and continuously modify the fuzzy inference system for a number of times in search for an optimal solution. The integral of absolute error:

$$IAE = \int_0^t \left| e(t)dt \right| \tag{29}$$

used as a measure of the system performance since, it is known to give a better all round performance indicator of a control system response where overshoot, settling time and rise time are the main considerations (Ko *et al*., 2006; Bucci *et al*., 2000). The initial settings for the operation of the GA should be defined. In this study, the population size, termination generation, crossover probability and mutation probability are given by Table 2.

The fitness value of the chromosome is the inverse of the performance indices. The fitness value is used to select the best solution in the population to the parent and to the offspring that will comprise the next generations. The fitter the parent greater is the probability of selection. This emulates the evolutionary process of survival of the fittest. Parents are selected using Roulette Wheel Selection Method.

Fitness function is reciprocal of performance indices. In this study, researches have taken the discrete form of ITAE. ITAE is treated as performance indices and fitness function denoted by J can be described as:

$$J = \frac{1}{\left(100 + \sum_{K=1}^{N} |\omega_{ref} - \omega_{m}|\right)} \quad (30)$$

SIMULATION RESULTS

The closed loop simulation using FLC and GA-FLC for L-type ZCS QRC , M-type ZCS QRC and ZVS QRC are carried out using MATLAB/Simulink Software. The harmonic spectrum of L-type ZCS QRC, M-type ZCS QRC and ZVS QRC with FLC and GA-FLC are shown in Fig. 8-13, respectively. Depending on error and the change in error, the value of change of switching frequency is calculated.

The fuzzy controller and GA-FLC has been designed and simulated wave forms of armature voltage, armature current and speed response are obtained. The fuzzy controller performance was also compared with GA-FLC performance for the converters. It has been inferred from the waveforms of speed response that the overshoot and settling time is less for FLC then compared to GA-FLC. Obviously it is a know fact that the performance of the converters with FLC is better than the conventional PI controllers. Again the closed loop response is good when compared with open loop where response is oscillatory. In this study, the analysis of harmonics in armature

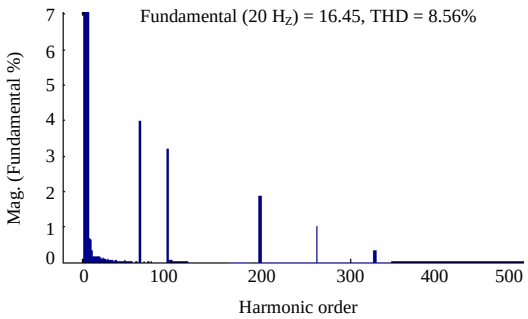

Fig. 8: Harmonic spectrum of L-type ZCS QRC with FLC

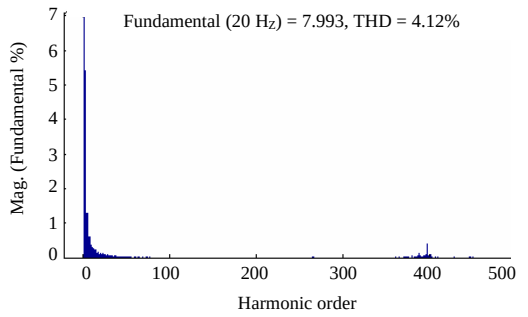

Fig. 9: Harmonic spectrum of L-type ZCS QRC with GA-FLC

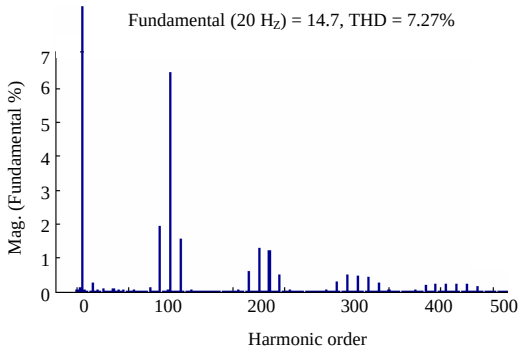

Fig. 10: Harmonic spectrum of M-type ZCS QRC with FLC

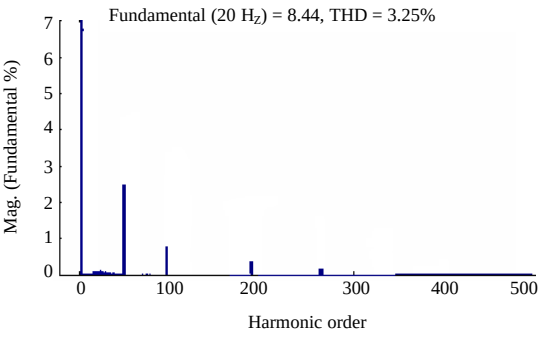

Fig. 11: Harmonic spectrum of M-type ZCS QRC with GA-FLC

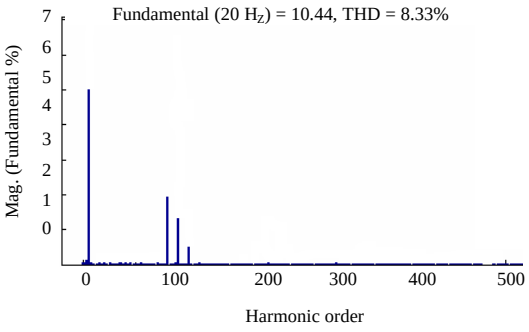

Fig. 12: Harmonic spectrum of ZVS QRC with FLC

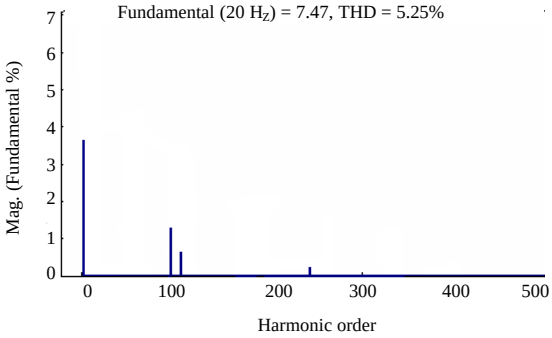

Fig. 13: Harmonic spectrum of ZVS QRC with GA-FLC

Table 3: Harmonic spectrum analysis of various converters

Converters	Fundamental	THD
L-type ZCS QRC		
FLC	16.450	8.56
FLC-GA	07.993	4.12
M-type ZCS QRC		
FLC	14.700	7.27
FLC-GA	08.440	3.45
ZVS QRC		
FLC	10.440	8.33
FLC-GA	7.470	5.25

current waveform for ZCS QRC and ZVS QRC fedby FLC and GA-FLC are inferred. The fundamental component and THD for various QRC's are presented in Table 3.

CONCLUSION

Applications of FLC and GA-FLC for the converters like Series (L-type) ZCS QRC, Parallel (M-type) ZCS QRC and ZVS QRC fed dc drive are modeled and simulated are presented. The harmonic analysis of the above said converters has also been carried out in this study. It has been inferred that in order to obtain high performance and reduction of THD the parameters of FLC should be optimized. To avoid getting stuck in local optimum, GA is used in this paper to search the optimal solution. The results demonstrate that the controller after optimized by GA yields the following merits: faster response with reduced overshoot, a short settling time, reduced IAE which means that the steady state error. The total harmonic distortion is reduced compared to the FLC. This promises in the application of the GA-FLC technique when employed for various types of converters fed dc drive provides better performance with reduced harmonic disturbances when employed in control applications.

REFERENCES

Arulselvi, S. and U. Govindarajan, 2007. Real time implementation of modified Fuzzy logic controller for a non linear quasi resonant DC-DC converter. IETE J. Res., 53: 401-416.

Balestroni, A., A. Landi and L. Sani, 2000. Cuk converter global control via fuzzy logic and scaling factors. IEEE Trans. Ind. Appl., 147: 107-112.

Bose, B.K., 1994. Expert system, fuzzy logic and neural network Applications in power electronics and motion control. Proc. IEEE, 82: 1303-1323.

Bucci, G., M. Faccio and C. Landi, 2000. New ADC with piecewise linear characteristics: Case study-implementation of a smart humidity sensor. IEEE Trans. Instrument Measure., 49: 1154-1166.

Hu, B.G., G.K.I. Mann and R.G. Gosine, 1997. Theoretic and genetic design of a three-rule fuzzy PI controller Proceedings of 6th IEEE International Conference on Fuzzy Systemss, Jul. 1-5, Barcelona, Spain, pp: 489-496.

Kandel, A. and G. Langholz, 1994. Fuzzy Control Systems. CRC Press, Boca Raton.

Ko, C.N., T.L. Lee, Y.Y. Fu and C.J. Wu, 2006. Simultaneous auto-tunning of membership functions and fuzzy control rules using gentic algorithms. Proceedings of the IEEE International Coference on Systems, Man and Cybernetics, October 8-11, 2006, IEEE Computer Society, USA, pp: 1102-1107.

Kung, Y.S. and C.M. Liaw, 1994. A fuzzy controller improving a linear model following controller for motor drive. IEEE Trans. Fuzzy Syst., 2: 194-202.

Liu, K.H. and F.C.Y. Lee, 1990. Zero- voltage switching technique in K/DC converters. IEEE Trans. Power Electron., 5: 293-304.

Mattavelli, P., L. Rossetto, G. Spiazzi and P. Tenti, 1997. General-purpose fuzzy logic controller for dc-dc converters. IEEE Trans. Power Electron., 12: 79-86.

Mohammadian, M. and R.J. Stonier, 1994. Generating fuzzy rules by genetic algorithms. Proceedings of the 3rd IEEE International Workshop on Robot and Human Communication, July 18-20, 1994, Nagoya, pp: 362-367.

Mohan, N., T.M. Undeland and W.P. Robbins, 1995. Power Electronics Conveiters, Application and Design. 2nd Edn., John Wiley and Sons, New York.

Reznik, L., 1997. Evolution of fuzzy controller design. IEEE Trans. Fuzzy Syst., 2: 503-508.

Tan, G.V. and X. Hu, 1997. More on designing fuzzy controllers using genetic algorithms: Guided constrained optimization. IEEE Trans. Fuzzy Syst., 1: 497-502.